Theory/experiments of X-Ray flux effect on periodic lattice distortions in $YBCO_{7-\delta}$

J.V. Acrivos and H.S. Sahibudeen
San José State University, San José CA95192-0101

ABSTRACT

The effect of X-ray flux on periodic lattice distortion waves in $YBa_2Cu_3O_{7-\delta}$, $YBCO_{7-\delta}$ 50nm films, on $SrTiO_3$, is described: The flux r(ft)=d[photons]/dt induces resonant excitations: $h\nu+YBa_2Cu_3O_{7-\delta}\rightarrow X^{\neq}$ that indicate a path for the transition: $YBCO_{7,metal}\Leftrightarrow X^{\neq}\Leftrightarrow YBCO_{6.5,insulator}$. The mole fraction, y_{YBCOx} at r(ft) (determined by inserting Al filters ft t mil thick) obeys the relation: $1/y_{YBCO}=1 + r(ft)\ T_1$ (fig. 1) where T_1 is the $X^{\neq}$ lifetime and $1/T_1$ is of order $r(f0)\sim10^{10}$/s achieved in synchrotrons. ***Figure 1**: 1-12 XRD at 8.048keV, Ω=0, 298K versus $\phi-\phi_0$ at different incident photon rates, r(ft). Insert shows the experimental fit $1/y_{YBCO}=S(\infty)/S(t)$ versus r(ft)/r(f0) to obtain $T_{1,(1-12)}=0.4/r(f0)$.*

Keywords: Nano-particle SCF calculation, periodic lattice distortions, nano-film synchrotron radiation XAS and XRD.

1. INTRODUCTION

A study of YBCO nano films, important for industrial applications, compares phenomena in films to bulk crystals.

2. EXPERIMENTAL

50 nm YBCO epitaxial films, grown by sputtering in an oxygen atmosphere on a $SrTiO_3$, STO 100 plane, with and without a 24DEG ab grain boundary, GB at the Complutense University[1a,b] were characterized by plane polarized synchrotron photon energy 7 to 9.5keV XRD at SSRL-7-2 at 298K (fig. 1-3) and by 001 enhanced scattering (I_s/I_0) collected at LBNL-ALS-6.3.1 at 0.5 to 2 keV in the Kortright chamber at different temperatures[1c-e, 2] (fig. 4, 8) and distinguished from fluorescence (F/I_0) and total electron yield (TEY/I_0) in the Nachimuthu chamber[1c-e, 3]. E was calibrated at E(CuO, Cu:L_3)=931.2eV[1d]. Samples are identified by the STO substrate single crystal, SC or two fused with a 24° ab GB, BC qualified by the year fabricated/year measured. The O composition is ascertained from bulk crystal XRD data[4,5]. The incident plane polarized beam $\mathbf{I_i}=\{k_i,\varepsilon_i,h_i\}$ 10 by 100μm wide, intensity I_0, on the $1cm^2$ film at x (fig. 2 insert) makes an angle θ to the scattering plane and 2θ' to the scattered beam $\mathbf{I_f}=\{k_f,\varepsilon_f,h_f\}$ detected versus $\mathbf{s}=\{s_0,0,0\}+d\mathbf{s}$, $s_0=\sqrt{(H^2/a_0^2+K^2/b_0^2+L^2/c_0^2)}=2\sin\theta_0/\lambda$ and the CTS/monitor record the intensity of the momentum transfer $\mathbf{Q}=k_f-k_i=s_0\{-\cos(\theta'-\theta),\sin(\theta-\theta'),0\}$[4j] versus θ, χ, ϕ (fig.1-4). Then:

$$d\mathbf{s}=s_0\{\cot\theta,1,0\}d\theta,\ s_0\{0,0,d\chi\},\ \text{and}\ s_0\{0,\cos\chi,0\}d\phi \qquad (1)$$

versus Δθ, Δϕ with $2\theta'=2*\theta_{Bragg}$, and ΔH=-ΔK scans obtain H,K,L≠0 XRD with sidebands sb to the center-band cb (fig.1-3), $\phi_0=\text{atan}(a_0K/b_0H)+C$, $\chi_0=\pi/2+\text{acos}(L/c_0/s_0)$. Inverse rotations obtain the orientation dependent amplitudes ε

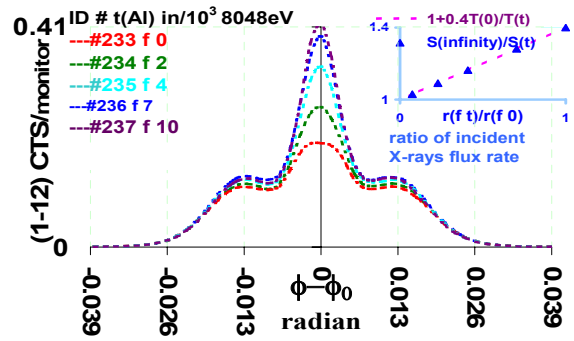

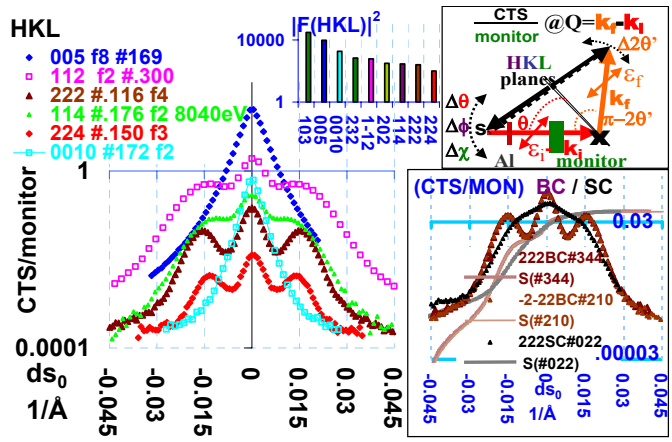

Figure 2: 298K YBCO BC04/04 50nm film XRD semi-log CTS per monitored incident beam intensity with Al filters ft, t''/10³ thick versus $ds_0=2(\sin\theta-\sin\theta_0)/\lambda$, E=8.04keV. Inserts show: $|F(HKL)|^2$ for D^{17}_{2h} YBCO to identify the structure, the sample geometry, and the SC film superimposed on the resolved BC film 222 XRD-PLD.

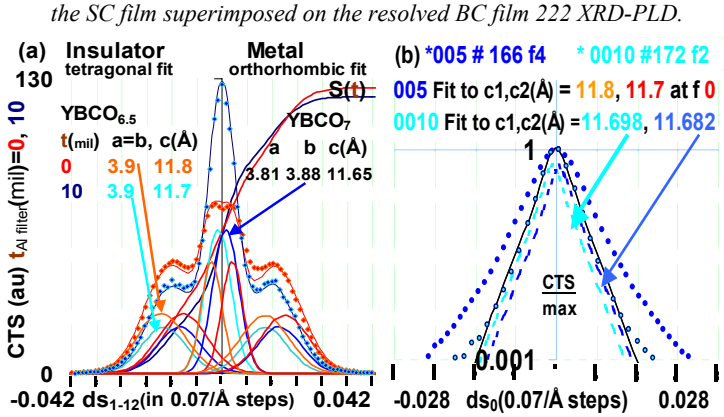

*Figure 3: XRD scans versus θ fitted to two phases at 298K: **(a)** 1-12 XRD, t=0 and 10 mil identify an unchanged orthorhombic phase plus a tetragonal (a=b,c)→(3.89,11.69Å) as t increases, equally abundant phases. **(b)** 0010 XRD Lorentzian line shapes (HWHH≈0.08 DEG) convoluted with a Gaussian (HWHH~0.3 DEG) for the phases determined in **(a)**. The $sb_{\pm1}$ maxima at $q_x=\pm q_y\approx a^2 s_0\ ds_{sb\pm1}/2H\approx1/24$ (fig. 2, 3a), obtained the PLD vector[1b,d1], agreeing with dK, -dH scans that determine the diagonal $q_{xy}=(dK_0/K-dH_0/H)_{sb\pm1}\approx2^{-½}/24$, H,K,L≠0 (fig. 8).*

along the a,b,c crystal axes, and project d**s** into the reciprocal lattice axes[4i] that plot the rocking curves versus the respective abscissa (fig. 2-4). When $\varepsilon=\varepsilon_i\approx\varepsilon_f$, $k=k_i\approx k_f$, $\mathbf{I_f}=\{k_f \sin(2\theta'-\theta) - \varepsilon_f \cos(2\theta'-\theta)), k_f \cos(2\theta'-\theta) + \varepsilon_f \sin(2\theta'-\theta), \hbar_f\}$.

The XRD integrated intensity S(t) at an incident X-ray flux r(ft) is proportional to the mole fraction of a given $YBCO_x$ phase detected at $\Omega=2\theta'-2*\theta_{Bragg}=0$ for the given HKL (fig. 1). The rate of incident photons r(ft) = d[hν]/dt = r(f0)T(0)/T(t), $r(f0)\approx10^{10}s^{-1}$ is decreased by inserting Al filters ft, t mil thick in the path of $\mathbf{I_i}$, (fig. 2) and counting for a time T(t) to achieve constant monitor counts versus t.

DISCUSSION OF RESULTS

The data analysis is based on the structure factor[4, 6a]:

$$F=\Sigma_j f_j(\mathbf{k_i}, \mathbf{k_f}, E)=\Sigma_j[\alpha_j f_j^o(\mathbf{k_i}, \mathbf{k_f})+\Delta f_j(\mathbf{k_i}, \mathbf{k_f}, \boldsymbol{\varepsilon_i}, \boldsymbol{\varepsilon_f}, E)]. \quad (2)$$

f_j^o leads to Bragg scattering, resonance effects are due to: $\Delta f_j \propto \Sigma_{nl}\langle\boldsymbol{\varepsilon_f}.\boldsymbol{\mu}_{ln}e^{-i\mathbf{k_f}.\mathbf{r_j}}\rangle\langle e^{i\mathbf{k_i}.\mathbf{r_j}}\boldsymbol{\mu}_{nl}.\boldsymbol{\varepsilon_i}\rangle/[(E_n-E_l-h\nu_{in}+\Delta_n)-iHWHH]$ plus its Hermitian conjugate, $\boldsymbol{\mu}_{ln}$ is the dipole matrix element between initial and final excited states n, l with energies E_n, E_l, the state lifetimes determine the half width at half height HWHH, $\alpha_j = \Sigma_j \exp(i(\mathbf{k_i}-\mathbf{k_f}).\mathbf{r_j})$ are the crystallographic site weights, Δ_n= Lamb shift. The relative sb to cb scattering intensity when a PLD displaces an atom *l* at $\mathbf{R}_{0l}$ to $\mathbf{R}_l=\mathbf{R}_{0l}+\boldsymbol{\delta}_l$ when $\boldsymbol{\delta}_l=\mathbf{u}_l \exp(i(2\pi\mathbf{R}_{0l}.\mathbf{q}+\varphi))$[1b,d,4a,g]:

$$\text{Area}_{\text{side-band, n=±1}}/\ \text{Area}_{\text{center band}}=|J_1(z_l)/J_0(z_l)|^2, \quad (3)$$

is non-zero when $(\mathbf{s}+n\mathbf{q}).(\mathbf{R}_l-\mathbf{R}_{l-1})$ and n are integers, $z_l=2\pi\,\mathbf{u}_l.\mathbf{s}$ and J_n are ordinary Bessel functions (fig.1-3). H±HL XRD-PLD obtain $\mathbf{q} \approx \pm(1,-1,\sim0)/24$, $\mathbf{u} \geq 0.04$ (a,-b,~0) (fig. 2) that describes YBCO twin formation where the angles $\mathbf{b}\hat{}\mathbf{a}$ = 90°±0.02% and atan(b/a) = 45.05°±0.12% remain constant along one plane diagonal forming stripes as shown below (fig. 5, 6). The SC film 222 XRD superimposes on the BC sideband structure (fig.2 insert) where the integral S shows inflection points at ds_0=-0.30/Å for sb_{-2} suggests that PLD are present also on SC but resolved only in BC films.

Important evidence for the rate of exchange between at least two phases is obtained as follows: **i.** The dependence of HKL scattered intensity S(t) versus the incident X-ray flux at 8.048keV indicates that resonance excitations to an activated complex $X^{\neq}$ (fig. 1) determines the detected YBCO mole fraction at $\Omega=2\theta'-2*\theta_{Bragg}=0$: $y_{YBCO}=S(t)/S(\infty)$, and at steady state obtains:

$$-dy_{YBCO}/dt = r(ft)\ y_{YBCO}= dy_{YBCO}/dt =(1-y_{YBCO})/T_1,$$

$$1/y_{YBCO} = S(\infty)/S(t) = 1 + T_1\ r(ft) \quad (4)$$

where $1/T_1(005)=0.2r(f0)$ is slower than $1/T_1(1\text{-}12)=2.5r(f0)$ (fig.1), and $|F(005)/F(1\text{-}12)| \approx10$ suggests that the $X^{\neq}$ lifetime T_1 depends on E, ε and the total scattering cross section, and therefore may be due to resonance transitions near 8040 to 8048eV (eq. 2). Then $1/T_1$ is equal to the sum of the Einstein induced and spontaneous emission rates that leads to a steady state equilibrium:

$$YBa_2Cu_3O_{7,\ metal} \Leftrightarrow X^{\neq} \Leftrightarrow YBa_2Cu_3O_{\leq6.5,\ insulator}. \quad (5)$$

where $\Delta E_{nl}^{-1}|\boldsymbol{\mu}_{nl}.\boldsymbol{\varepsilon}_{1\text{-}12}|^2/\Delta E_{n'l'}^{-1}|\boldsymbol{\mu}_{n'l'}.\boldsymbol{\varepsilon}_{005}|^2\approx10$ are the relative transition probabilities due to resonance effects[6c] and,

$\{\varepsilon_a^2+\varepsilon_b^2,\varepsilon_c^2\}/\varepsilon^2\} = \{0.8,0.2\}_{1\text{-}12,8048eV}$; $\{0.1,0.9\}_{005,8040eV}$, but these were not observed at 7, 8 or 9.5keV. **ii.** The 1-12 $sb_{\pm1}$ and 0010, 005 XRD (fig. 3) may be fitted to at least two phases with a Lorentzian line shape, with $(HWHH)_L \leq 0.1$DEG, convoluted in order to fit the wings with a Gaussian, $(HWHH)_G\simeq0.4$DEG that indicates a broadening of $2\pi\mathbf{s}$ by $\Delta k=4\pi(HWHH)_G/\lambda\simeq 0.04$/Å due to a dynamic exchange rate $\omega\approx (k_BT/m_O)^{½}\Delta k \geq 10^{10}s^{-1} \approx 1/T_1$ (for m_O=O atomic mass) as described in liquids[4e]. Thus $X^{\neq}$ at 298K is an intermediate between at least two equally abundant metal and insulator phases enhanced by X-ray resonance effects in the soft YBCO film, but may also be an intermediate in other phase transitions, e.g., versus T.

Enhanced scattering I_s/I_0 was used to determine that more than one phase is present in the film[1d]. Hanzen[5a] has correlated the O composition in $YBCO_{7-\delta}$ with the unit cell c_i. Energy shifts in the 001 I_s/I_0 enhanced peak (fig. 4, at fixed θ, 2θ') indicate the presence of different c_i phases as the incident beam scans the film surface near a GB. Here:

$$\Delta c_i/c_i\approx-\Delta E_{Bragg}/E_{Bragg} \quad (6)$$

follows from the 001 Bragg relation, and $E_{Bragg}>E(O_{K\text{-}edge})$ obtains f^0 as a baseline correction leading to I_s/I_0 (eq. 2, fig. 4) similar to the $O_{K\text{-}edge}$ XAS[1d, 6c,7]. Farther than 100 μm from the GB, a peak at E_{Bragg} =545eV obtains c_i =11.7Å for the ortho-I $YBCO_{\sim6.9}$, but the growth of a new enhancement peak within 100μm of the GB, at ~540eV indicates in addition the presence of a higher $c_{i,GB}\approx11.8$Å for $YBCO_{\leq6.5}$. The 8% O composition decrease in this phase may be due to flux heating and dynamic plastic interfacial strain[4c,d,m 5d,e].

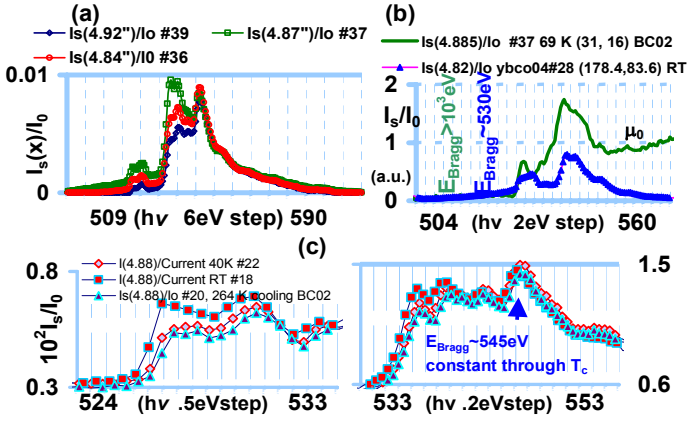

Figure 4: *Enhanced 001 I_s/I_0 scattering near the O:K edge for BC02/03, BC04/04:* ***(a)*** *At different beam position* ***x*** *near the GB .* ***(b)****For different values of E_{Bragg} normalized to XAFS: $\mu_0 = 1 = \alpha_{O:1}$.* ***(c)*** *Constant I_s/I_0 peak observed at E_{Bragg} = 545 eV indicates there is no c_i change through T_c.*

001 I_s/I_0 at different $E_{Bragg}=E(O_{K\text{-}edge})+DE$ correlate with the bulk XAS[5a,6c](fig. 4), but in addition since (2) depends on the crystallographic weights $\alpha(\mathbf{k_i}-\mathbf{k_f})$ (Table **I**) the transition:

$$O{:}1s^2..\Leftrightarrow O{:}1s..np_{x,y},\ \ O{:}1s^2..\Leftrightarrow O{:}1s..np_z,\ n>2 \quad (7)$$

NSTI-Nanotech 2007, www.nsti.org, ISBN 1420061828 Vol. 1, 2007

changes in I_s/I_0 from DE=0 to 1500eV identify the O:i site edges by the changes in α(O:i): **i.** The O:2 edge is near 528-δ by the doubling of α(O:2). **ii.** The O:1 edge is near 528+δ to 530eV by the constant intensity as α(O:2)/α(O:1) = 0.8, 1.9 sharpening below T_c and. **iii.** The $O{:}3_{A,B}$ edge is near 531- 535eV by the sign changes in $\alpha(O{:}3_{A,B})$ vs DE: $I_s/I_0(\alpha(O{:}3_{A,B},DE=1.5keV)\approx 3.2)>0$, $I_s/I_0(\alpha(O{:}3_{A,B},DE=0)\approx -2.8)\leq 0$. These assignments, obtained earlier by XAS and XPE[6c, 7] in the bulk crystal indicate that the O atoms electro-negativity/ shielding varies in the YBCO lattice: If the O:1 and O:2 sites are occupied by O^{-2} ions then $O{:}3_{A,B}$ are occupied by $O^{-(0\ to \leq 1)}$ and CuO_2 is a covalent conduction layer as graphite. Also, since the effect of X-ray flux depends on HKL where $|\Sigma f_O\alpha_{O:3A,B}|/|\Sigma f_{Cu}\alpha_{Cu2}|_{HKL=005}\approx 2$, $|\Sigma f_O\alpha_{O:3A,B}|/|\Sigma f_{Cu}\alpha_{Cu2}|_{HKL=112}\approx 0.1$ correlate with $T_{1,005}/T_{1,112}\approx 10$, this suggests that $X^{\neq}$ is produced by excitations of delocalized states near the Fermi energy dominated by $O{:}3_{AB}$ electron density. The early SCF calculations for Cu_4O_4 in a YBCO crystal field indicated that the $HOMO_{MO74}$ shows a continuous electron density along the diagonal $O_A{:}O_B$ σ-bonds, while Cu is weakly bonding (fig. 5a)[8a] and lead to a CuO_2 layer extended state chains:

$$\Psi_{HOMO,k}=\Sigma_i e^{i\mathbf{k}.\mathbf{R_i}}(a(O_{Ai}{:}2p_{xy}-O_{Bi}{:}2p_{xy})+bCu_i{:}3d_{xy})/\sqrt{N} \qquad (8)$$

where for $\mathbf{k}=\mathbf{k_F}=\pm(\pi,\pm\pi,0)$ show a constant $O{:}2p_{xy}$ overlap $\langle e^{i\mathbf{k}.\mathbf{R_A}}O_{Ai}{:}2p|e^{-i\mathbf{k}.\mathbf{R_B}}O_{Bi}{:}2p\rangle$ greater than zero along an in plane ab diagonal, which focuses 1D transport along that $(O_A{:}O_B)_{1/2q}$ chain. To change the overlap direction a chain bond must be broken at the cost of an excitation energy, $h\nu_{ex}\sim|t|/N$, N=1/q, where t≈-260meV is the single bond exchange integral[5f] forming bi-radicals $(O_{3A}\text{-}O_{3B})_{N/2}^{=}\equiv X^{\neq}$. This explains the $YBCO_7$ orthorhombic to tetragonal phase transition at 700K[5g] when q=1/4, but at lower T and q_{PLD}= 1/24, |t|/N= 3017/24 =125K. At 298K, $X^{\neq}$ decays at a rate $1/T_1$ into the two equally populated phases observed, but at 125 K the charge vortices produced by the PLD (fig. 5b) can lead to BKT transitions[8d,e] where lattice vibrations focus 1D superconductivity along that in plane diagonal, as found in the bulk[5b,f,g]. Overhauser has already suggested that PLD effects may lead to superconductivity[4g].

*Table**I**: Crystallographic weights $\alpha=\cos(\mathbf{Q}.\mathbf{r})$[5a,6a] used in (2) for $YBa_2Cu_3O_{7-\delta}$, D^{17}_{2h}: $\alpha_M(001)=n_M\cos(2\pi z_M E/E_{Bragg})$ where $E_==E_{Bragg}=E(M_{edge})$, $E_{\neq}=E(M_{edge})=E_{Bragg}-DE(eV)$ (fig. 4b, 8), and n_M= number of equivalent M≡O,Cu,Y,Ba.*

M SITE:	x(a)	y(b)	z(c)
O:1/Cu:1	0/ ½	½/ ½	0/ 0
Ba/O:2	0/ ½	0/ ½	.18/ .16
Cu:2	½	½	.36
O:3A/3B	½/ 0	0/ ½	.38/ .38
Y:	0	0	½
$\alpha_{O:K}(001)$	O: 1	2	3A+3B
$E_{Bragg}=E_=$	1	1.0	-2.8
$1500+E_=$	1	1.9	3.2
$\alpha_{Cu:L23}(001)$Cu:		1	2
$E_=$		1	-1.3
$150+E_=$		1	-0.7

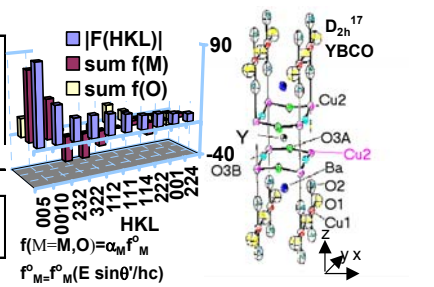

$f(M=M,O)=\alpha_M f^o_M$

$f^o_M=f^o_M(E\sin\theta'/hc)$

$\alpha_M=n_M\cos((k_f-k_i).r_M)=n_M\cos(4\pi E z_M c_i\sin\theta'/hc)$

$\alpha_M = n_M\cos(2\pi z_M E/E_{Bragg})$

(a) Cu_4O_4 HOMO: (**b**) CuO_4 unit cell twist by **q**:

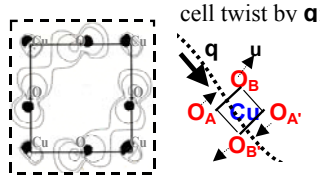

***Figure 5:** Possible PLD source and effects: **(a)** Electron density in Cu_4O_4 HOMO: $\rho_e \geq 10^{-3}b^{-3}$ [8a]. **(b)** Transverse $\mathbf{q}_{PLD}$ (3) that produces twins and O_4 twists giving rise to charge vortices.*

The physical significance of **q** in the film properties may be different from the bulk crystal. However, the observed PLD compare to the additional XRD reciprocal lattice spots assigned to twinning in single crystals[4k] and explain the stripes observed in TEM by the periodicity of $O_A{\cdot}O_A\hat{}O_B{\cdot}O_B=90^o\pm0.02^o$ and $O_A{\cdot}O_A\hat{}O_AO_B=45.05^o\pm0.6^o$ in the CuO_4 angles (fig. 5) which remain unchanged only along one ab diagonal (fig. 6) causing an elastic strain $\varepsilon_{(01)} = 1 - \tan(O_A{\cdot}O_A\hat{}O_AO_B/2) = -.07\%$ that leads to a preferred twin[4m] with possible film buckling and/or stripes[6d].

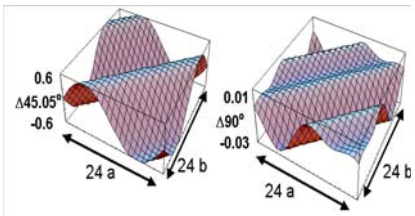

***Figure 6:** Deviation from $O_A{\cdot}O_A\hat{}O_AO_B$ = atan(b_0/a_0) = 45.05° and $O_A{\cdot}O_A\hat{}O_B{\cdot}O_B$ = 90° due to PLD on Cu_4O_4 (fig. 5b).*

States near the Fermi energy will interact via the absorption and emission of photons at resonance. Given[4f],

$$E=E(Ba_{L3\text{-}edge})+E(Ba_{M3\text{-}edge})+E(Ba_{M4\text{-}edge})+E(Cu_{L3\text{-}edge})=8042eV, \quad (9)$$

states in YBCO have a finite cross section for $h\nu_{in}$=8048 to 8040eV. Then $h\nu_{out}=h\nu_{in}-E$ can induce $\Psi_{HOMO,\mathbf{k}=\pm(\pi,\pm\pi,0)}$ (fig. 7)[8a] absorption which transfers $\mathbf{k}_F\text{-}\mathbf{k}_{free} \parallel \mathbf{q}$ to the scattering vector $\mathbf{Q}=\mathbf{k}_i\text{-}\mathbf{k}_f$[8f,g]. Thus resonance can and does enhance the sideband amplitude and BKT vortices[8d,e]. But, since

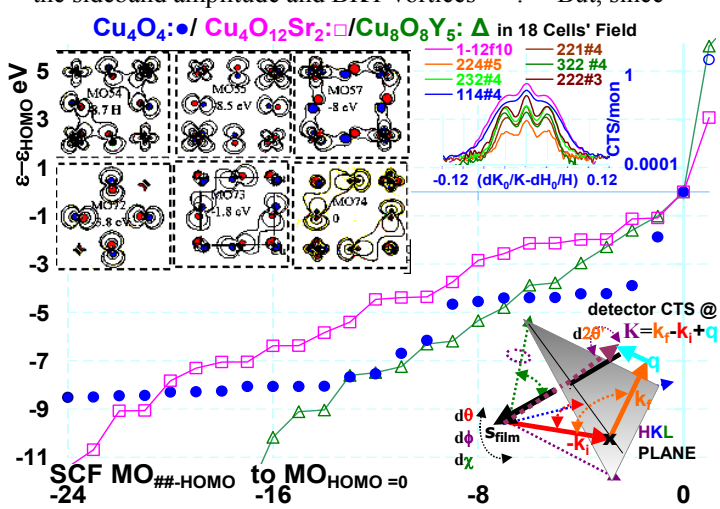

***Figure 7:** Exact SCF MO basis near the Fermi level for different size lamella in 18 unit cells' crystal field with similar energy up to $\varepsilon\text{-}\varepsilon_{HOMO}\approx$-8eV. Inserts show: the tight binding approximation (8) MO basis with anti-parallel alignment of two diagonal $3d^9Cu$, s=1/2, $m(d_{x2-y2})$ atoms in the $HOMO_{MO74}$[8a], how excitations of (8) add $\mathbf{k}_F\text{-}\mathbf{k}_{free} \parallel \mathbf{q}$ to $\mathbf{Q}=\mathbf{k}_f\text{-}\mathbf{k}_i$, and XRD plots showing coincident $sb_{\pm1}$ that obtain $q_{xy}=(dK_0/K\text{-}dH_0/H)_{sb\pm1}\approx 2^{-1/2}/24$ in all H,K,L≠0 d(H-K) scans.*

XRD sidebands due to **q** obtain **u**~0.04(a,-b,0) independent of r(ft) when $h\nu_{in}$=7.2, 8.0 and 9.5keV, the PLD appear to be an intrinsic film property where only the amplitude increases in the presence of resonance excitations.

I_s/I_0 peaks enhanced near the $Cu_{L3,L2}$ edge (fig. 8) as $E \Rightarrow E_{Bragg}$ indicate the complexity of the transitions[7b,c]:

$$.Cu{:}2p_{3/2}. \Leftrightarrow .Cu{:}3d_{5/2}. \quad \text{and} \quad .Cu{:}2p_{1/2}. \Leftrightarrow .Cu{:}3d_{3/2}. \quad (10)$$

Now the advantage of I_s/I_0 over XAS is evident. The Cu:1,2 site contributions are identified by the opposite sign of α in the D^{17}_{D2h} group (Table **I**). Less shielding by 0.65±0.05eV is detected at Cu:1 than at Cu:2 sites more convincingly than by Cu XAS[7c, 8b-d]. Below T_c a shift of 0.6±0.05eV and an increase in the Cu:1 peak integrated intensity definitely confirms the formation of X-ray polarons, excitons and/ or new vacancies in Cu:1 3d final states[7c]. The $O_{K\text{-edge}}$ measurements indicate that the O atom shielding changes are of the order of ~0.2eV below T_c (fig. 4c) and transfer $\mathbf{k}_{valence}$-$\mathbf{k}_{free}$ from $\Psi_{\mathbf{HOMO,k}=\pm(\pi,\pm\pi,0)}$ by excitation at hν= $k_BT = |t|/N$ near 125K for N=24 and |t|=260meV[5f] as first suggested by the SCF calculations $HOMO_{MO74}$[8a] and first discovered experimentally by XPE[8h] in bulk crystals.

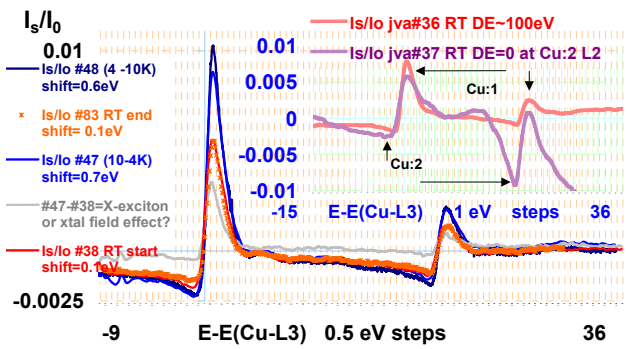

Figure 8: *BC04/04 Cu:$L_{2,3}$ edges I_s/I_0(x = 5.02, θ = 29.5, 2θ' = 65.5°, E_{Bragg}-E(Cu_{L3})=150eV) extremes of reversible 12h temperature cycle. Far from the edge, baselines were made to coincide, and the 4-10K energy scale was shifted by 0.65±0.05eV with respect to the RT for all to coincide at E-E(Cu-$L_{3,2}$)=0. Insert identifies peaks associated with atoms at Cu:i sites by the opposite sign of α(Cu:i, i=1,2)[6a] (Table* I*) showing strong enhancement effects as E⇒E_{Bragg}.*

4. CONCLUSION

Results obtained using synchrotron radiation measurements indicate that in fabricated $YBCO_x$ soft solid nano-films, PLD are present in SC though resolved only in BC films, and XRD resonance effects identify a path for the metal insulator transitions (5) between phases that are also found in bulk YBCO where the intermediate in (5) $X^{\neq}$ may be associated with $(O_A{:}O_B)_{1/2q}^{=}$ bi-radical chains formed when changing the direction of diagonal conductivity by resonance X-ray flux effects and/ or by temperature T.

5. ACKNOWLEDGEMENTS

Supported by NSF and Dreyfus Foundations at SJSU, by DOE at SSRL and LBNL-ALS. Thanks are due to all scholars working to solve some YBCO puzzles[1-8].

REFERENCES

[1](a) M.A. Navacerrada, et al., *Europhys. Lett* **54**, 387 (2001); (b) M.A. Navacerrada and J.V. Acrivos, *NanoTech2003*, **1**, 751 (2003); (c) H.S. Sahibudeen, et al., *Nanotech 2005*, **2**, 573 (2005); (d) J.V. Acrivos, http://arxiv.org/cond-mat/0510003; (e) M.A. Navacerrada et al., Mat. Res. Soc. Symp. Proc. Vol.868E, C8.2.1 (2005)

[2] J.B. Kortright et al., *J. Magn. Magn. Materials*, **207**, 7 (1999)

[3]P.Nachimuthu et al., *Chem. Mater.* **15**, 3939 (2003)

[4] (a) R.W. James, "*The optical principles of X-rays*", OxBow Press, 1949, 1962; (b) L.K. Templeton and D.H. Templeton, *Acta Cryst. A* **47**, 414 (1991); (c) F.R.N. Nabarro, "*Theory of crystal dislocations*", Dover, NY (1967); (d) B.D. Cullity and S.R. Stock, "*Elements of XRD*" Prentice Hall (1994); (e) U. Balucani and M. Zoppi, *"ynamics of the Liquid State"*, Oxford Press (1994); (f) f° Cromer–Mann atomic scattering coefficients obtained from Center for X-Ray Optics data, http://www.cxro.lbl.gov; (g) A.W. Overhauser, *Phys. Rev. B* **10**, 3173 (1971); *Phys. Rev. Lett,* **61**, 1885 (1988); (h) V.M. Agranovich and V. Ginsburg, "*Crystal Optics*", Springer-Verlag, Berlin (1984); (i) W.R. Busing and H.A.Levy, *Acta Cyst* **22**, 457 (1967); (j) F. Oscelli et al., *Phys. Rev. B.* **63**, 224306 (2000); (k) G.J.McIntyre, *ibid,* **37**, 5148 (1988); (l) J.Dow et al., *ibid,* **69**, 174505 (2004); (m) J. Brötz et al., *ibid,* **57**, 3679 (1998)

[5](a) R.M. Hanzen et al., "*Physical Properties of High Temperature Superconductors, II*" World Scientific (1990), p.121; (b) C. Thomsen et al., *ibid,* p. 409; (c) N.H. Andersen, *Physica C,* **317-318**, 259 (1999); (d) J. Brötz et al., *Phys. Rev. B*, **57**, 3679 (1998); (e) C.Cantoni et al., *ibid.,* **71**, 054509 (2005); (f) T. Zhou et al., *ibid.* **69**, 224514 (2004); **72**, 134512 (2005); (g) J.D.Jorgensen et al., *ibid.* **36**, 3608 (1987); (h) S.Kittelberger et al., *Physica C*, **302**, 93 (1998); (i) G.Cannelli et al., *Supercond. Sci. Technol.* **5**, 247 (1992); (j) S.Degoy, et al., *ibid, C,* **256**, 291 (1996)

[6](a) L.B. Sorensen et al., *"Diffraction anomalous fine structure"* North Holland, G. Materlik et al., ed (1994) p.389; (b) J.H. Guo et al., *Phys. Rev. B* **61,** 9140 (2000); (c)Y. Ma et al., *ibid*, **49**, 5799 (1994); (d) E.A.Jagla, *ibid,* **75**, 085405 (2007)

[7] (a) A. Bianconi et al, *Phys. Rev.B* **38,** R7196 (1988); (b) F.M.F. deGroot et al., *ibid.* **42,** 5459 (1990); (c) J.V. Acrivos et al., http://arxiv.org/cond-mat/0504369

[8](a) J.V. Acrivos and O. Stradella, *International Journal of Quantum Chemistry*, **46**, 55 (1993); (b) J.V. Acrivos, *Solid State Sciences*, **2**, 807 (2000); (c) J.V. Acrivos et al., *Microchemical Journal,* **71**, 117 (2002); (d) *ibid.* **81**, 98 (2005); (d) V.I. Berezinskii, *Zh.Eksp.Teor.Fiz* **59**, 907*(1970);* (e) J.M. Kosterlitz and D.J. Thouless, *J.Phys.C,* **5**, L124 (1972); (f) T. Åberg et al., *J. Phys.* **B** 15, L435 (1982); *Phys. Rev.* **A**, **27**, 3375 (1983); *Phys. Rev. Lett,* **54,** 1142 (1982)]; (g) Y. Ma, *Phys. Rev. B* **49**, 5799 (1994); *Phys.Rev. Lett.* **74**, 478 (1995); (h) Z-X Shen, W.E.Spicer, et al., Science **267**, 343 (1995)